Journal of
Synchrotron
Radiation

ISSN 1600-5775

Received 28 August 2013
Accepted 24 October 2013

Numerical reconstruction of an object image using an X-ray dynamical diffraction Fraunhofer hologram

Minas K. Balyan

Faculty of Physics, Department of Solid State Physics, Yerevan State University, Alex Manoogian 1, Yerevan 0025, Armenia. E-mail: mbalyan@ysu.am

A numerical method of reconstruction of an object image using an X-ray dynamical diffraction Fraunhofer hologram is presented. Analytical approximation methods and numerical methods of iteration are discussed. An example of a reconstruction of an image of a cylindrical beryllium wire is considered. The results of analytical approximation and zero-order iteration coincide with exact values of the amplitude complex transmission coefficient of the object as predicted by the resolution limit of the scheme, except near the edges of the object. Calculations of the first- and second-order iterations improve the result at the edges of the object. This method can be applied for determination of the complex amplitude transmission coefficient of amplitude as well as phase objects. It can be used in X-ray microscopy.

Keywords: X-ray Fraunhofer holography; X-ray dynamical diffraction; X-ray microscopy; image processing.

1. Introduction

In the work of Balyan (2013), an X-ray dynamical diffraction Fraunhofer holographic scheme was proposed and theoretically investigated. It was shown that, by illuminating an X-ray dynamical diffraction Fraunhofer hologram with visible light, an object image can be reconstructed. In the mentioned work the corresponding references are given as well.

Numerical methods of reconstruction are important for phase objects (Snigirev *et al.*, 1995; Momose, 1995). In this work we briefly describe the scheme mentioned above (Balyan, 2013) and then discuss a numerical method of reconstruction of an object image. As an example, the image reconstruction of a circular cylindrical beryllium wire is presented.

2. Brief description of an X-ray dynamical diffraction Fraunhofer hologram recording

In Fig. 1 an X-ray dynamical diffraction Fraunhofer hologram recording scheme is shown. An object is placed in the path of an incident plane monochromatic X-ray wave with unit amplitude. In a thick perfect crystal (of thickness T), under the condition of two-wave dynamical Laue-case symmetrical diffraction, the reference plane wave and the object wave interfere on the exit surface of the crystal and an interference pattern is formed. By recording this interference pattern in the diffracted field, one obtains an X-ray dynamical diffraction Fraunhofer hologram of the object. The crystal is sufficiently thick and only the weakly absorbing mode of σ-polarization can be taken into account. The intensity distribution of the diffracted wave is (Balyan, 2013)

$$I_h = |E_h|^2 = |E_{h\,\mathrm{ref}}|^2 + E_{h\,\mathrm{ref}}E^*_{h\,\mathrm{obj}} + E^*_{h\,\mathrm{ref}}E_{h\,\mathrm{obj}} + |E_{h\,\mathrm{obj}}|^2, \quad (1)$$

where $E_{h\,\mathrm{ref}}$ is the amplitude of the reference wave and $E_{h\,\mathrm{obj}}$ is the amplitude of the object wave. The third term of the right-hand side after reconstruction gives the real direct image of the object and the second term gives the virtual image of the object.

3. Numerical reconstruction of an object image

The analytical analyses given by Balyan (2013) show that by multiplying (1) by $\exp[i\pi(p - x)^2/(2D)]$ (the coordinate axes

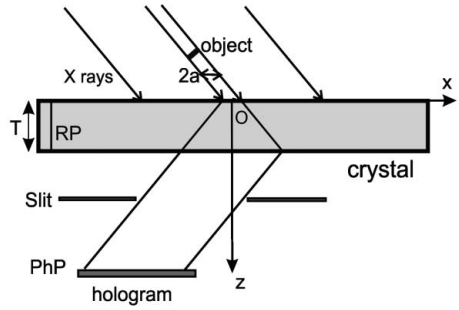

Figure 1
X-ray dynamical diffraction Fraunhofer hologram recording scheme. RP, reflecting planes; PhP, photographic plate. The axes of the coordinate system are shown.

in the diffraction plane are shown in the Fig. 1) and integrating by x over the hologram plane the numerical reconstruction of the object image can be obtained. Here p is a parameter and $D = \Lambda T \tan^2\theta$, where Λ is the extinction length and θ is the Bragg angle. We assume that the experimental values of I_h are known. After integration one can write

$$E_{\rm rec} = \sum_{j=1}^{4} E_{{\rm rec}\,j}, \tag{2}$$

where

$$E_{\rm rec} = \int_{x_1}^{x_2} I_h(x,y)\exp\left[i\pi(p-x)^2/(2D)\right]{\rm d}x, \tag{3}$$

$$E_{\rm rec\,1} = \int_{x_1}^{x_2} \left|E_{h\,\rm ref}\right|^2\exp\left[i\pi(p-x)^2/(2D)\right]{\rm d}x, \tag{4}$$

$$E_{\rm rec\,2} = \int_{x_1}^{x_2} E_{h\,\rm ref}E^*_{h\,\rm obj}\exp\left[i\pi(p-x)^2/(2D)\right]{\rm d}x, \tag{5}$$

$$E_{\rm rec\,3} = \int_{x_1}^{x_2} E^*_{h\,\rm ref}E_{h\,\rm obj}\exp\left[i\pi(p-x)^2/(2D)\right]{\rm d}x, \tag{6}$$

$$E_{\rm rec\,4} = \int_{x_1}^{x_2} \left|E_{h\,\rm obj}\right|^2\exp\left[i\pi(p-x)^2/(2D)\right]{\rm d}x. \tag{7}$$

Here $x_2 = T\tan\theta - a_{\rm obj}$, $x_1 = -x_2$ are coordinates of the bounds of the hologram in the diffraction plane, and $a_{\rm obj}$ is half of the object size in the diffraction plane along the Ox axis. Our purpose is to reconstruct the amplitude complex transmission coefficient $t(x, y)$ of the object (y is the coordinate counting perpendicular to the diffraction plane). Note that $E_{\rm rec}$ and $E_{\rm rec\,1}$ are known but $E_{\rm rec\,2}$, $E_{\rm rec\,3}$ and $E_{\rm rec\,4}$ are unknown. We have an integral equation (2) for $t(x, y)$.

3.1. Analytical approximation

This mathematical procedure of image reconstruction is equivalent to image reconstruction by visible light on the focusing plane of the real image. In this plane $E_{\rm rec\,2,4}$ can be neglected. According to Balyan (2013), as the result of integration an approximate expression for the object amplitude complex transmission coefficient t can be found,

$$t(p + k\cos\theta\Delta\theta D/\pi, y) \simeq E_{\rm rec}(p, y)/E_{\rm rec\,1\infty}. \tag{8}$$

Here k is the wavenumber, $\Delta\theta$ is the deviation from the exact Bragg angle (it is assumed that the deviation from the exact Bragg angle is not large and the influence of $\Delta\theta$ on the amplitude can be neglected),

$$\begin{aligned} E_{\rm rec\,1\infty} &= \int_{-\infty}^{+\infty} \left|E_{h\,\rm ref}\right|^2\exp\left[i\pi(p-x)^2/(2D)\right]{\rm d}x \\ &= (D/8)^{1/2}\exp\left[-\mu_{\rm d}T/(2\cos\theta) + i\pi/4\right], \end{aligned} \tag{9}$$

the subscript ∞ of $E_{\rm rec\,1\infty}$ means that in (4), instead of x_1, x_2, the infinite integral limits of the integral are taken, and $\mu_{\rm d}$ is the diffraction linear absorption coefficient of the crystal. The parameter p is varied in the limits $-a_{\rm obj} - k\cos\theta\Delta\theta D/\pi \leq p \leq a_{\rm obj} - k\cos\theta\Delta\theta D/\pi$. Thus, according to (8),

$$t(x, y) \simeq E_{\rm rec}(x - k\cos\theta\Delta\theta D/\pi, y)/E_{\rm rec\,1\infty}, \tag{10}$$

and x is varied in the limits $-a_{\rm obj} \leq x \leq a_{\rm obj}$. An example will be considered below (§4).

3.2. Image reconstruction by numerical method of iterations

For more detailed and precise reconstruction an iteration procedure is necessary. $E_{h\,\rm obj}$ is a convolution along the entrance surface of the crystal of the point source function and the amplitude of the incident wave (see Balyan, 2013). For zero-order approximation, ignoring $E_{\rm rec\,2,4}$ in (2) and in the expression of $E_{h\,\rm obj}$ under the integral sign of convolution expanding $S(x', y) = 1 - t(x', y)$ into Tailor series around the point $x_0(p) = p + k\cos\theta\Delta\theta D/\pi$, taking only the first term of the expansion, *i.e.* $S(x', y) = S^{(0)}[x_0(p), y]$, and taking out $S^{(0)}[x_0(p), y]$ under the integral sign in (6) and using (2), one can find

$$\begin{aligned} t^{(0)}(x, y) = 1 - &\left[E_{\rm rec}(x - k\cos\theta\Delta\theta D/\pi, y) - E_{\rm rec\,1}\right] \\ &/E_{\rm rec\,3\,abs}(x - k\cos\theta\Delta\theta D/\pi, y). \end{aligned} \tag{11}$$

In (11), $E_{\rm rec\,3\,abs}$ is $E_{\rm rec\,3}$ for a completely absorbing object [for such an object $t(x, y) = 0$] of the same size as the considered object. In all of the terms on the right-hand side of (11) the integration is performed in the finite limits x_1, x_2.

For the first-order approximation in the expression of $E_{h\,\rm obj}$ under the integral sign of the convolution we expand $S(x', y)$ into Tailor series around the point $x_0(p)$ including linear terms, *i.e.* $S(x', y) = S^{(1)}[x_0(p)] + S^{(0)\prime}[x_0(p)][x' - x_0(p)]$, where $S^{(0)\prime}[x_0(p)]$ is the approximate value of the derivative of $S(x', y)$ with respect to x' at the point $x' = x_0(p)$. Using now (2) and taking out $S^{(1)}[x_0(p)]$ under the integral sign in (6) one can find

$$\begin{aligned} t^{(1)}(x, y) = t^{(0)}(x, y) - &t^{(0)\prime}(x, y)\,E^{(1)}_{\rm rec\,3}(x - k\cos\theta\Delta\theta D/\pi, y) \\ &/E_{\rm rec\,3\,abs}(x - k\cos\theta\Delta\theta D/\pi, y), \end{aligned} \tag{12}$$

where $E^{(1)}_{\rm rec\,3}(x - k\cos\theta\Delta\theta D/\pi, y)$ is $E_{\rm rec\,3}(x - k\cos\theta\Delta\theta D/\pi, y)$ in which $S(x', y)$ is replaced by the linear $S(x', y) = x' - x_0(p)$.

For the second-order approximation in the expression of $E_{h\,\rm obj}$ under the integral sign of convolution of the expression of $E_{h\,\rm obj}$ we expand $S(x', y)$ into Tailor series around the point $x_0(p)$ including quadratic terms, *i.e.* $S(x', y) = S^{(2)}[x_0(p)] + S^{(1)\prime}[x_0(p)][x' - x_0(p)] + S^{(1)\prime\prime}[x_0(p)][x' - x_0(p)]^2/2$. Using once again (2) and taking out $S^{(2)}[x_0(p)]$ under the integral sign in (6) one can find

$$\begin{aligned} t^{(2)}(x, y) = t^{(0)}&(x, y) \\ &- \left[t^{(1)\prime}(x, y)E^{(1)}_{\rm rec\,3}(x - k\cos\theta\Delta\theta D/\pi, y)\right. \\ &\left./E_{\rm rec\,3\,abs}(x - k\cos\theta\Delta\theta D/\pi, y)\right] \\ &- \left[t^{(1)\prime\prime}(x, y)E^{(2)}_{\rm rec\,3}(x - k\cos\theta\Delta\theta D/\pi, y)\right. \\ &\left./2E_{\rm rec\,3\,abs}(x - k\cos\theta\Delta\theta D/\pi, y)\right], \end{aligned} \tag{13}$$

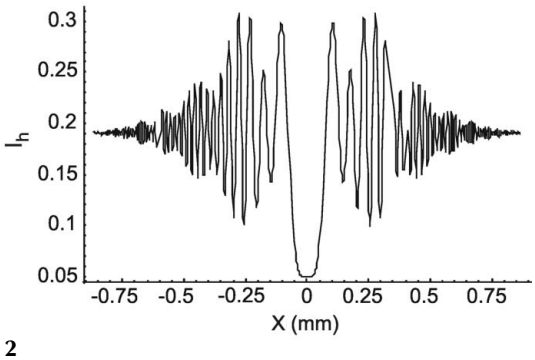

Figure 2
Intensity distribution on the dynamical diffraction Fraunhofer hologram of the beryllium wire.

where $E^{(2)}_{\mathrm{rec}\,3}(x - k\cos\theta\Delta\theta D/\pi, y)$ is $E_{\mathrm{rec}\,3}(x - k\cos\theta\Delta\theta D/\pi, y)$ with the quadratic $S(x', y) = [x' - x_0(p)]^2$. The iteration procedure can be continued. A corresponding example will be considered in the next section.

4. Example

Let us consider an example, *i.e.* the case of a Si(220) reflection, with $\lambda = 0.71$ Å (17.46 keV) radiation, $\Delta\theta = 0$, $T = 5$ mm, σ-polarization is taken, and $\mu T = 7.3$. As an object we take a circular cylindrical beryllium wire, with the axis perpendicular to the diffraction plane. The radius R_{obj} of the wire $R_{\mathrm{obj}} = a_{\mathrm{obj}}/\cos\theta = 30$ µm. The refractive index of beryllium is $n = 1 - \delta + i\beta$, where $\delta > 0$ and defines the refraction, $\beta > 0$ defines the absorption. For beryllium, $\delta = 1.118 \times 10^{-6}$, $\beta = 2.69 \times 10^{-10}$ (Grigoryan *et al.*, 2010). The complex amplitude transmission coefficient is

$$t(x, y) = \exp\left[-2ik(\delta - i\beta)\left(R^2_{\mathrm{obj}} - x^2\cos^2\theta\right)^{1/2}\right]. \qquad (14)$$

Now we must numerically reconstruct (14) using the numerical methods described above. Using (14) we can calculate the intensity distribution on the Fraunhofer hologram of the considered object. In Fig. 2 the calculated intensity distribution on the hologram is shown. We take the values of the calculated intensity as the experimentally measured known values. Using these values, according to (10), one can calculate the analytical approximate values of $t(x)$. In Figs. 3(*a*) and 3(*b*) the results of calculations are compared with the real and imaginary parts of the exact values (14). According to Balyan (2013), the resolution of the scheme for the considered example is about 8 µm. This means that the obtained result coincides with the exact value predicted by the estimated value of the resolution. Near the edges of the object $t(x)$ varies rapidly and the limit of the resolution is not sufficient for reconstruction. Using the method of iterations described above one can improve the obtained result near the edges of the object also. In Figs. 4(*a*) and 4(*b*), Figs. 5(*a*) and 5(*b*), and Figs. 6(*a*) and 6(*b*) the real and imaginary parts of the zero-order, first-order and second-order iterations [calculated according to formulas (11), (12) and (13) accordingly], respectively, are compared with the real and imaginary parts of the exact values of $t(x)$. The second-order iteration values

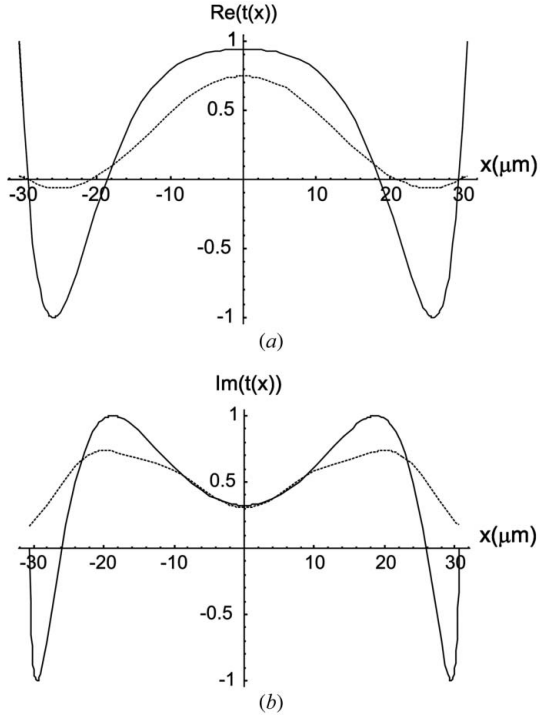

Figure 3
Comparison of the reconstructed analytical approximation with exact amplitude complex transmission coefficient of the beryllium wire. (*a*) Real parts: solid line, exact values; dashed line, analytical approximation. (*b*) Imaginary parts: solid line, exact values; dashed line, analytical approximation.

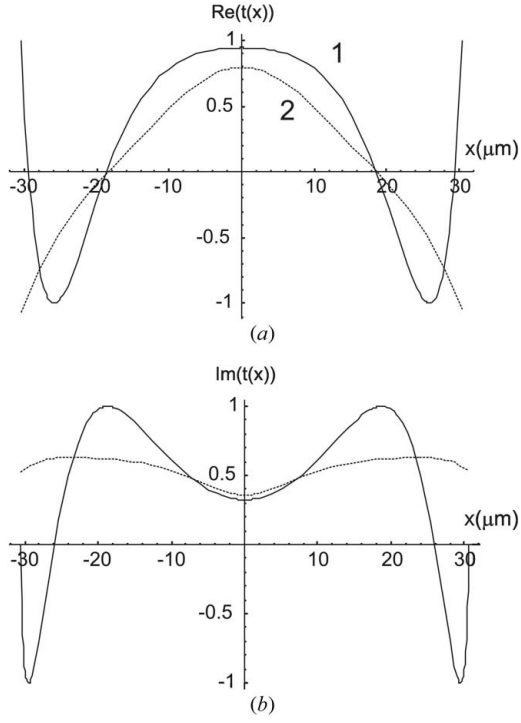

Figure 4
Comparison of the reconstructed zero-order iteration with the exact amplitude complex transmission coefficient of the beryllium wire. (*a*) Real parts: solid line, exact values; dashed line, zero-order iteration. (*b*) Imaginary parts: solid line, exact values; dashed line, zero-order iteration.

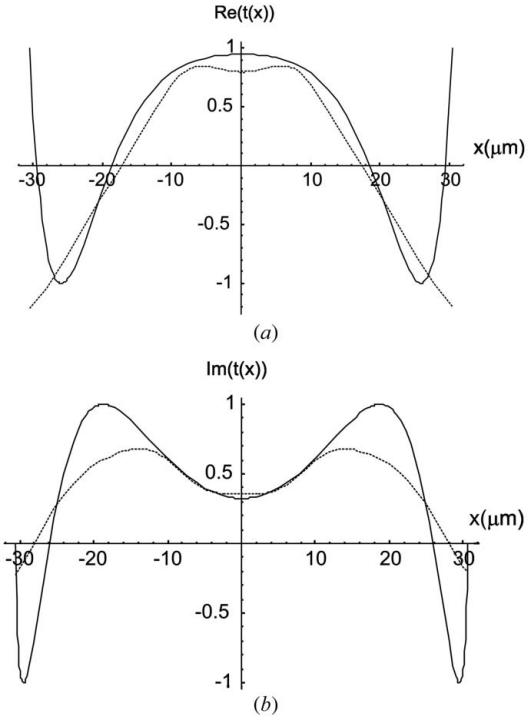

Figure 5
Comparison of the reconstructed first-order iteration with the exact amplitude complex transmission coefficient of the beryllium wire. (*a*) Real parts: solid line, exact values; dashed line, first-order iteration. (*b*) Imaginary parts: solid line, exact values; dashed line, first-order iteration.

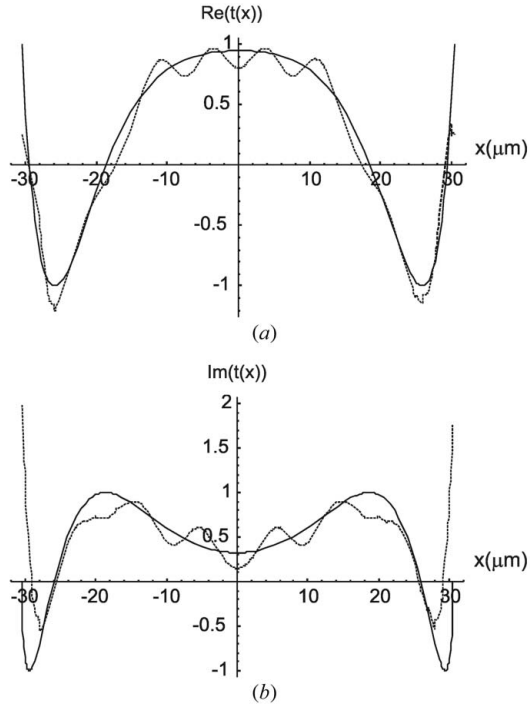

Figure 6
Comparison of the reconstructed second-order iteration with the exact amplitude complex transmission coefficient of the beryllium wire. (*a*) Real parts: solid line, exact values; dashed line, second-order iteration. (*b*) Imaginary parts: solid line, exact values; dashed line, second-order iteration.

have non-physical oscillating character. This is partially avoided by taking the average of $t^{(2)}(x)$ and $t^{(1)}(x)$. In Figs. 6(*a*) and 6(*b*) the second-order iteration values correspond to $\bar{t}^{(2)}(x) = [t^{(2)}(x) + t^{(1)}(x)]/2$. As can be seen in Figs. 4, 5 and 6, the object complex amplitude transmission coefficient is reconstructed also near the edges of the object, where the resolution is not sufficient for reconstruction. The non-physical oscillations of the second-order iteration can be avoided by averaging the obtained values.

5. Conclusion

In this paper a numerical method of an object image reconstruction using an X-ray dynamical diffraction Fraunhofer hologram is presented. Methods of analytical approximation and numerical methods of iterations are discussed. An example of a reconstruction of an image of a cylindrical beryllium wire is considered. The results of analytical approximation and zero-order iteration coincide with exact values of the amplitude complex transmission coefficient of the object (except near the edges of the object) as predicted by the resolution limit of the scheme. Calculations of the first- and the second-order iterations improve the result near the edges of the object.

This method can be applied for determination of the complex amplitude transmission coefficients of amplitude as well as phase objects. It can be used in X-ray microscopy.

Further development of this method could use an asymmetrical reflection or an X-ray LLL interferometer.

References

Balyan, M. (2013). *J. Synchrotron Rad.* **20**, 749–755.
Grigoryan, A. H., Balyan, M. K. & Toneyan, A. H. (2010). *J. Synchrotron Rad.* **17**, 332–347.
Momose, A. (1995). *Nucl. Instrum. Methods Phys. Res. A*, **352**, 622–628.
Snigirev, A., Snigireva, I., Kohn, V., Kuznetsov, S. & Schelokov, I. (1995). *Rev. Sci. Instrum.* **68**, 5486–5492.